Gomes *et al.*
EJNMMI Radiopharmacy and Chemistry (2025) 10:11
https://doi.org/10.1186/s41181-025-00334-x

EJNMMI Radiopharmacy and Chemistry

RESEARCH ARTICLE Open Access

High-efficiency [^{18}F]fluoride pre-concentration using a laser-micromachined anion-exchange micro-cartridge

Antonio Arleques Gomes[1*], Arian Pérez Nario[1], André Luis Lapolli[1], Ricardo Elgul Samad[1], Emerson Soares Bernardes[1] and Wagner de Rossi[1]

*Correspondence:
antonio.gomes@usp.br;
gomesbjj.33@gmail.com

[1] Instituto de Pesquisas Energéticas e Nucleares (IPEN-CNEN—SP), São Paulo, SP CEP 05508–000, Brazil

Abstract

Background: The use of radiopharmaceuticals labelled with fluorine-18 in non-invasive imaging, particularly in Positron Emission Tomography (PET), increased significantly during the last decade. However, traditional nucleophilic fluorination synthesis methods in most cases require azeotropic drying steps, leading to loss of activity and increased synthesis time. Microfluidic devices offer improvements with shorter reaction times, higher elution efficiency, and reduced reagent quantities.

Results: We developed a novel micro-cartridge for [^{18}F]fluoride trapping and elution, etched in borosilicate optical glass (BK7) using ultrashort laser pulse machining. The micro-cartridge has a bead volume of 17 µL and a maximum capacity of 8.5 mg for anion exchange resin. The micro-cartridge, without the need for QMA preconditioning, exhibited an overall trapping efficiency and recovery efficiency (RE) of (94.09 ± 0.12)% using an activity exceeding 123 GBq of [^{18}F]fluoride. This RE was obtained using 100 µL of a standard solution of anhydrous acetonitrile with Kryptofix 2.2.2, containing only 5 µL of water and 5.4 µmol of K_2CO_3 for [^{18}F] fluoride elution. This solution was employed directly in the radiosynthesis of [^{18}F] fluoromisonidazole ([^{18}F]FMISO), resulting in a 100% radiochemical conversion (RCC) to THP-protected [^{18}F]FMISO within 10 min at 110 °C.

Conclusions: The developed micro-cartridge provides a novel tool for integrating microfluidic chips into conventional cassettes, facilitating more efficient radiopharmaceutical preparation.

Keywords: Microfluidics, Micro-cartridge, [^{18}F]fluoride, Positron emission tomography (PET), Ultra-short laser pulse

Background

Positron Emission Tomography (PET) is a powerful, non-invasive imaging tool used to assess metabolic activity in vivo with high sensitivity, providing good image quality, short scan times, and the ability to analyze dynamic biological processes (Vallabhajosula 2007; Rahmim and Zaidi 2008; Berg and Cherry 2018; Zhang et al. 2020). The [^{18}F]fluoride is the preferred radionuclide for PET due to its favorable chemical and physical

properties, including low positron energy (0.635 MeV) and a half-life of 109.7 min. This extended half-life allows ample time for labeling molecules and enables the study of biological processes lasting over 100 min, outperforming shorter-lived PET radionuclides like Carbon-11 (^{11}C, 20.4 min) and Oxygen-15 (^{15}O, 2.04 min) (Jacobson et al. 2015; Haveman et al. 2023).

Standard aqueous [^{18}F]fluoride production typically uses automated synthesis modules with cassette-based processes (Vallabhajosula 2009; Krasikova 2007). The production begins with pre-concentration, where aqueous [^{18}F]fluoride from a cyclotron is trapped on an anion exchange resin (commonly a Waters Sep-Pak QMA) and then eluted with an acetonitrile solution containing a base and a cryptand, usually K_2CO_3/Kryptofix 2.2.2, at up to 50% water content (Vallabhajosula 2009; Krasikova 2007; Yu 2006; Scott 2015). However, this high-water content in the eluate requires azeotropic drying to create anhydrous [^{18}F]fluoride for nucleophilic fluorination synthesis (Hamacher et al. 1986; Brichard and Aigbirhio 2014; Pees et al. 2018; Zhang et al. 2018b, 2019). This drying step presents significant limitations: (1) It is time-intensive (10–15 min) and can result in notable radioactivity loss ($\leq$30%); (2) It complicates automated modules; and (3) If drying fails or the [^{18}F]fluoride is insufficiently anhydrous, radiolabeling yield is reduced, potentially causing synthesis failure (Haveman et al. 2023; Pees et al. 2018; Zhou et al. 2023).

To overcome these issues, microfluidic technologies have gained considerable interest (Pascali et al. 2013; Lisova et al. 2021; Zhang et al. 2018a; Elizarov et al. 2010; Lee et al. 2005). Microfluidics offer reduced reaction volumes, faster reaction times due to higher surface-to-volume ratios, and decreased reagent consumption and costs in radiopharmaceutical production (Sushanta and Mitra 2012; Panigrahi 2016; Knapp et al. 2020; Ovdiichuk et al. 2021). Accordingly, research efforts have increasingly focused on microreactors for azeotropic drying and radiolabeling in [^{18}F]fluoride synthesis (Elizarov et al. 2010; Lebedev et al. 2013; Chao et al. 2018), with commercial micro-cartridges like Opti-Lynx™ (5 µL particle bed volume) being widely used (Lebedev et al. 2013; Chao et al. 2018). Given its significant importance and demand, other groups have focused on developing custom micro-cartridges for [^{18}F]fluoride pre-concentration in the microfluidic synthesis of radiopharmaceuticals (Zhang et al. 2018a; Leonardis et al. 2011; Pascali et al. 2011; Salvador et al. 2017).

Despite these advancements, most conventional methods still use azeotropic drying except for (Chao et al. 2018), prompting development of alternative nucleophilic fluorination approaches without azeotropic drying. Studies have shown that eluting [^{18}F]fluoride with low water content ($\leq$10%) in microfluidic synthesis is feasible (Vallabhajosula 2009; Arima et al. 2013; Pascali et al. 2014; Hoover et al. 2016), and recent methods report success with nucleophilic [^{18}F]fluoride synthesis under hydrated conditions ($\leq$5% water), eliminating the drying step entirely (Ovdiichuk et al. 2024). The micro-cartridge design is crucial for implementing these hydrated methodologies.

The choice of material for microfluidic devices is influenced by its physicochemical properties, the precision required in chip design, and the expected conditions (e.g., pressure, temperature, solvent compatibility) (Niculescu et al. 2021). Traditionally, soft lithography, particularly with Polydimethylsiloxane (PDMS), has been extensively used in microfluidics for radiopharmaceutical applications (Zhang et al. 2018a; Elizarov

et al. 2010; Lebedev et al. 2013; Chao et al. 2018; Leonardis et al. 2011; Salvador et al. 2017). However, PDMS exhibits drawbacks with alcohols or organic solvents used for recovery or drying of [^{18}F]fluoride (Elizarov et al. 2010; Chao et al. 2018), leading to the search of alternative materials and manufacturing techniques. Laser ablation has thus emerged as a suitable choice, enabling precise, adaptable creation of microfluidic systems from diverse materials. Ultrashort laser pulses provide excellent precision, minimal heat-affected zones, and negligible physical or chemical alterations in surrounding areas (Waldbaur et al. 2011; Baker et al. 2011; Nolte et al. 2016; Juodenas et al. 2018). Among available materials, borosilicate glass (BK7) is advantageous for microfluidic development due to its cost-effectiveness, reproducibility, and physicochemical properties, making it suitable for applications in integrated optics and medical fields (Pawar et al. 2017; Shakeri et al. 2019).

This study presents the first micro-cartridge made from glass BK7 using ultrashort laser pulse micromachining, offering an efficient alternative for device production. Filled with QMA anion exchange resin, the micro-cartridge enables high-yield pre-concentration of [^{18}F]fluoride, demonstrating strong trapping and recovery efficiency across various activities. Experimental findings show effective [^{18}F]fluoride recovery with activities over 110 GBq. A hybrid synthesis approach, combining the micro-cartridge with a conventional method and eliminating the azeotropic drying step, achieved optimal radiochemical conversion (RCC) of fluorine-18 for THP-protected [^{18}F]Fluoromisonidazole ([^{18}F]FMISO) synthesis. This is the first report of micro-cartridge with RE activity exceeding 110 GBq and the largest RCC for the synthesis of [^{18}F]FMISO without azeotropic drying.

Methods

General

All reagents and solvents were commercially sourced from Sigma-Aldrich (Merck-Brazil) and used throughout the experiments without further purification. The resin used for packing the micro-cartridge in all experiments was extracted from Sep-Pak Plus Light QMA cartridges obtained from Waters (Brazil). Measurement of fluorine-18 radioactivity was conducted using a Capintec radioisotope dose calibrator (CRC-15R, New Jersey, USA), and analysis of the radiolabeled product by high-performance liquid chromatography (HPLC) was performed using an Agilent C18 column, (4.6 mm × 250 mm, 5 µm, 100 Å). The characterization of the micro-cartridge was carried out using a Zygo 3D optical profiler (ZeGage model).

Development and assembly of the anion exchange microfluidic cartridge

The micro-cartridge features a flat, vertically symmetrical design that includes an array of micropillars within the reservoir region. Each micropillar is machined to a depth of 312 µm and separated by 40 µm gaps, forming a sieve-like structure that retains the QMA resin in the reservoir while permitting fluids and gases to flow to the outlet channel. Both the resin reservoir and the inlet/outlet channels are 304 µm deep, so the micropillars extend slightly below the reservoir floor to facilitate liquid drainage. Micromachining was carried out using a titanium-sapphire (Ti) laser (800 nm, 30 fs pulse width, 10 kHz repetition rate) focused on a BK7 substrate attached to a 3D

translation stage with ± 10 nm positioning accuracy, applying a pulse energy of 17.5 μJ (Supplementary Fig. S1).

The cartridge assembly comprises three main components: (i) A laser-machined BK7 glass substrate, (ii) A 300 μm PDMS sheet, and (iii) An acrylic top plate, all sandwiched between an aluminum base plate and the acrylic top plate to form a watertight seal. Before final assembly is completed and for each new experiment, we manually pack the QMA resin into the micro-cartridge reservoir. Specifically, we use an acrylic mask—fabricated with the same geometry as the reservoir—to be placed over the laser-machined BK7 glass substrate. This mask is to aid in loading the resin into the reservoir and to prevent resin from leaking into the outlet channel during loading. After resin loading, the acrylic mask is removed and the cartridge is weighed in triplicate (before and after loading) to confirm the precise amount of QMA (Supplementary Fig. S2). The micro-cartridge is always used with fresh resin for each experiment, and no preconditioning is required. After each experiment, once the [^{18}F]fluoride activity has decayed (48 h for ≤ 10 GBq, 72 h for ≥ 74 GBq), the micro-cartridge is fully disassembled and the used resin discarded. The BK7 glass substrate and PDMS sheet are then cleaned (in line with cGRPP guidelines (Elsinga et al. 2010)), by rinsing three times with ultrapure water and isopropyl alcohol, plus a final acetone rinse for the BK7 substrate only. Both the PDMS sheet and the BK7 substrate are dried in an oven at 45 °C for 50 min. Repeated integrity checks, including microscopic inspection, profilometry, and flow rate tests, confirmed that neither the physical geometry nor the performance of the micro-cartridge was compromised after multiple cleaning cycles.

Production of no-carrier-added (n.c.a.) fluorine-18

No-carrier-added (n.c.a.) fluorine-18 was produced via the [^{18}O]oxygen (p,n) fluorine-18 e nuclear reaction from [^{18}O]H_2O (2.5 mL) (Rotem Industries Ltd, Hyox oxygen-18 enriched water, min. 98%), with protons beam of 18 MeV and integrated dose of 10 μAh (cyclotron, Cyclone-18, IBA).

Procedure for trapping and releasing of [^{18}F]fluoride

To assess trapping efficiency (TE) and recovery efficiency (RE), experiments were conducted with varying activities of fluorine-18, measured at the beginning of each experiment, in the micro-cartridge. For elution, a standard 5% water solution was prepared with 11.25 mg of K_2CO_3 in 75 μL Milli-Q water and 60.75 mg of Kryptofix 2.2.2 in 1425 μL anhydrous acetonitrile, stored at 4 °C for all experiments, including those with intermediate (≤ 10 GBq) and higher-activity (≥ 74 GBq).

For activities up to 10 GBq (using 1.5 mL of cyclotron material), experiments were conducted in a lead-shielded hood. Nitrogen gas was applied at (5.2 ± 0.6) psi to displace liquids during the trapping step and at (1.1 ± 0.3) psi during recovery. Following each step (trapping and recovery), a continuous nitrogen flow of (5.2 ± 0.6) psi was used to dry the reservoir for activity levels up to 10 GBq. For activities exceeding 74 GBq, nitrogen pressure ranged from (7.5 to 10.2 ± 0.3) psi. In higher-activity tests conducted in a hot cell, elution was performed at (1.1 ± 0.3) psi, while trapping and liquid removal required (7.5 to 10.2 ± 0.3) psi, adjusted for the 2.5 mL irradiated volume and the use of an extended ~ 150 cm flexible tube (Supplementary Figs. S5 and S6). All elution steps used 100 μL of the standard solution (5 μL

H_2O, 5.4 µmol K_2CO_3), except for one test each at intermediate and production-level activity, where a 50 µL total volume was employed (2.5 µL H_2O, 2.6 µmol K_2CO_3).

Radiosynthesis of [^{18}F]Fluoromisonidazole ([^{18}F]FMISO)

The [^{18}F]FMISO was synthesized via nucleophilic radiofluorination of the [^{18}F]fluoride ion with 1-(2′-nitro-1′-imidazolyl)-2-O-tetrahydropyranyl-3-O-tosyl-propanediol (NITTP) precursor following modified non-automated protocols similar to those reported in the literature (Patt et al. 1999; Sorger et al. 2003; Kämäräinen et al. 2004; Zheng et al. 2015), with adjustments in precursor mass, temperature, and reaction time, and without azeotropic drying. The [^{18}F]fluoride was eluted from the micro-cartridge with 100 µL directly into a 2 mL conical vial containing 4 mg of NITTP precursor in 400 µL of anhydrous acetonitrile (final volume 500 µL; 1% H_2O), and the mixture was heated for 10 min at 110 °C. After cooling, a high-performance liquid chromatography (HPLC) analysis was performed to assess radiochemical conversion (RCC). The mixture was then hydrolyzed with HCl (200 µL; 0.5 M) for 5 min at 100 °C, neutralized with NaOH (200 µL; 0.5 M), and analyzed again by HPLC to determine isolation efficiency (IE). The final product was purified through sequential Sep-Pak C18 and alumina (Al_2O_3) cartridges, washed with water, and then eluted with 5 mL of 10% ethanol into the collection vial, yielding purified [^{18}F]FMISO (Fig. 1).

Quality control

Aliquots of the THP-protected [^{18}F]FMISO and the final [^{18}F]FMISO (after deprotection by hydrolysis) were analyzed by HPLC to assess the process radiochemical conversion (RCC) and isolation efficiency (IE). The HPLC analysis was conducted under the following conditions: Stationary phase: Agilent C18 column, 4.6 mm×250 mm, 5 µm particle size, 100 Å pore size. Mobile phase: Solvent (A) Milli-Q water with 0.1% trifluoroacetic acid (TFA), Solvent (B) 100% acetonitrile (CH_3CN). Gradient elution: 0–100% B over 20 min. Flow rate: 1 mL/min and detection wavelength: 300 nm.

The radiochemical efficiency for each step (TE end RE) is calculated with the corrected activity decay, as follows:

$$TE = \left(\frac{micro - cartridge\ trapping}{micro - cartridge\ trapping + waste\ vial} \right) \times 100 \quad (1)$$

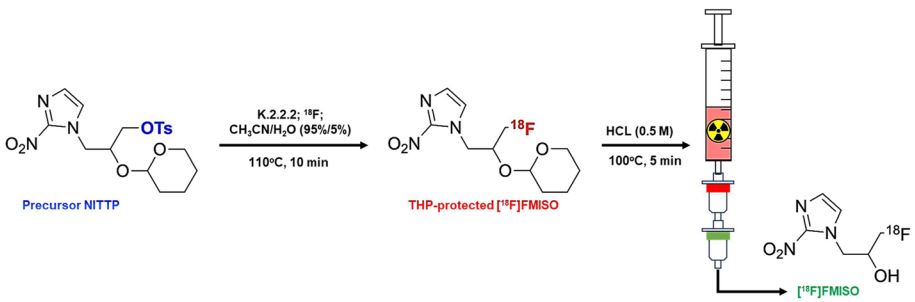

Fig. 1 Scheme Flowchart of [^{18}F]FMISO radiopharmaceutical synthesis

$$RE = \left(\frac{recovered\ vial}{micro - cartridge} \right) \times 100 \tag{2}$$

To determine the radiochemical yield (RCY) of the entire synthesis process, the consensus guidelines for radiopharmaceutical chemistry are followed (Herth et al. 2021). However, the resolubilization efficiency (RES) is excluded from the calculation, as the azeotropic drying step is not employed:

$$RCY = TE \times RE \times RCC \times IE \tag{3}$$

Results

Micromachining BK7 glass and assembly of the micro-cartridge

The micromachining of the BK7 glass micro-cartridge was executed in two stages to achieve precise geometrical features for optimal performance. In the first stage, the particle reservoir and inlet/outlet channels were machined to a depth of 304 µm using a 17.5 µJ laser pulses. In the second stage, 15 µJ pulses were used to machine micropillars with a depth of 312 µm, in order to ensure that the depth of the micropillars is slightly greater than that of the reservoir, allowing that when a gas flow passes through, all the liquid present in the reservoir is expelled to the outlet channel (Supplementary Table S1). The spacing between the micropillars is 40 µm, which is consistent with the average size distribution of QMA resin particles of (46 ± 9) µm. The etching parameters were determined in the same way as what was done for microfluidic mixers (Gomes et al. 2022). Also, the smooth ablation technique (Machado et al. 2011; Machado et al. 2012) was used to preserve the physical and chemical characteristics of the substrate. In the Fig. 2 shows photograph of the micro-cartridge and includes an optical profilometry analysis of one side of the outlet channel.

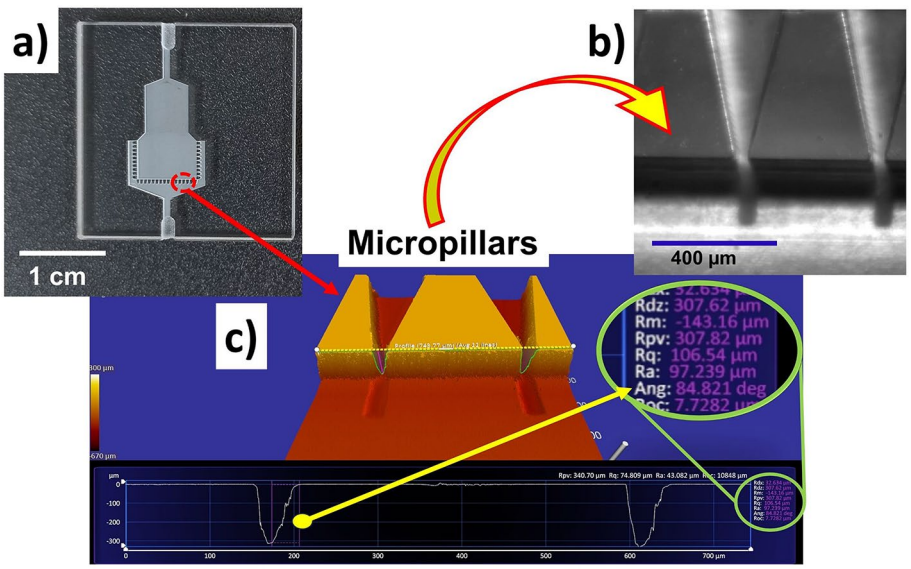

Fig. 2 **a** Photograph of the laser machined micro-cartridge; **b** Micrography of the micropillars; **c** Detailed profilometry of the micropillar structures showing wall inclination angles (Ang) and depth (Rdz)

Profilometry measurements (at least seven points) across the same micro-cartridge revealed an average pillar depth of (317 ± 10) µm—slightly exceeding the 304 µm reservoir depth—ensuring that residual fluid is expelled when a gas flow is applied. The mean spacing between pillars was (38.7 ± 0.8) µm, and the wall inclination angle was > 84°, indicating an almost vertical. We used Rdz to assess pillar depth accuracy and Ang to quantify the wall inclination, as these parameters provide critical insights into the structural fidelity of the micropillars and their impact on device performance. All these results highlight the high level of quality and geometric precision of the micro-cartridge achieved after the ablation process with the ultrashort laser pulse workstation. Furthermore, it is noteworthy that the excellent wall inclination results were obtained with a height/width ratio (h/w) greater than seven (Gomes et al. 2022).

The micro-cartridge assembly involved manually packing a new QMA resin for each experiment, always using an acrylic mask with a geometry matching the particle bed to prevent overflow into the outlet channel (Fig. 3b). After filling and compacting the resin into the reservoir, the acrylic mask was removed and replaced with a 3 mm thick PDMS layer to seal the micro-cartridge (Fig. 3a). Figure 3 Illustrates the assembly steps of the micro-cartridge. After weighing the QMA resin (Fig. 3c), the micro-cartridge pre-assembly pattern is used to determine the QMA mass. In the final configuration (Fig. 3d), all twelve screws are in place, forming a leak-tight seal.

The micro-cartridge reservoir, with a theoretical capacity of 8.5 mg for an approximate 17 µL particle bed, was loaded with an average of (7.6 ± 0.8) mg of QMA resin (n = 11), as summarized in Supplementary Table S2. Each loading event involved weighing the cartridge in triplicate (before and after) to confirm the resin mass. Under test conditions, the fully assembled micro-cartridge (Fig. 3d) showed no leakage at pressures exceeding 16 psi, confirming the reliability of the PDMS compression seal. A recent study using syringe-driven microfluidic pumps (Gomes et al. 2024), further demonstrated the micropillars' effectiveness in retaining the resin at flow rates up to 1000 µL/min (liquid) and 10,000 mm^3/min (compressed air), with no resin particles detected in the outlet channel.

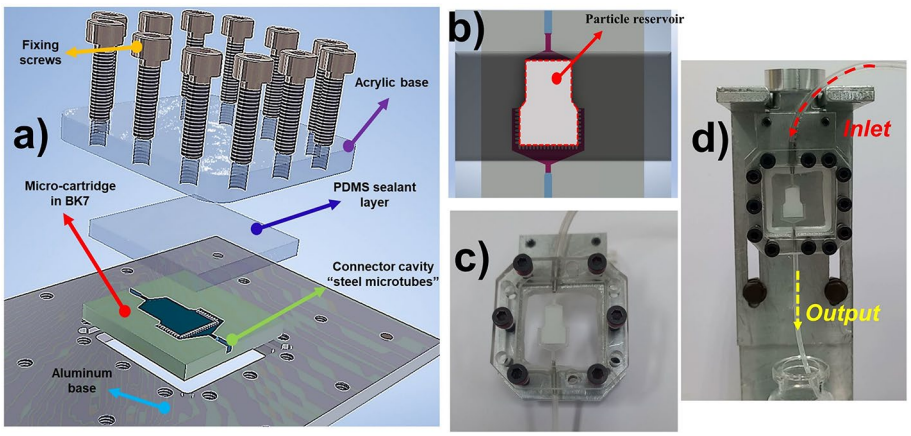

Fig. 3 **a** Representation of the sequence of the complete assembly of the micro cartridge; **b** Acrylic mask used to assist in packing the QMA resin; **c** Pre-assembly of the micro-cartridge for determination of the mass of QMA in the reservoir, always with the same screws in the same position; **d** Final assembly of the micro-cartridge with all the screws to form a watertight seal and the support used in the experiments

Our experiments showed no detectable leakage at pressures up to 16 psi, but for safety and prolonged device integrity, we recommend operating at < 14 psi for gas flow and up to 1.2 mL/min for liquids at the inlet connector (Supplementary Figs. S3 and S4). For high-activity tests (≥ 74 GBq) in a hot cell, we used ≤ 10.5 psi of N_2 to prevent unnecessary radiation exposure and to ensure consistent leak-free operation. Under these conditions, the measured activity before and after each run matched well with theoretical values, indicating negligible loss due to leaks.

Efficiency of trapping and elution of ^{18}F in micro-cartridge

The main focus of all tests on different activities in this work is to evaluate the efficiency of the micro-cartridge using a total volume of aqueous eluent of up to 100 µL containing a maximum of 5% water. Table 1 presents the performance of the micro-cartridge throughout all tests in the [^{18}F]fluoride pre-concentration process, with the efficiency results in the capture and recovery steps in intermediate activity (≤ 10 GBq).

Based on the results presented in Table 1, the micro-cartridge demonstrated a high efficiency during the capture and recovery stages, with an average efficiency of TE (98.2 ± 4.7)% and RE (98.7 ± 2.7)%. This was observed in all [^{18}F]fluoride pre-concentration processes, where a pressure flow of (5.2 ± 0.6) psi was used to displace 1.5 mL of liquid during the capture step, followed by (1.1 ± 0.6) psi in the recovery step. Additionally, between each step, a continuous N_2 flow was maintained at (5.2 ± 0.6) psi for 2 min and 1 min, respectively. The process, conducted in a fume hood with N_2 flow for liquid displacement and removal between the capture and recovery stages, was completed in an average time of (5.5 ± 0.5) minutes for the intermediate activity experimental setup (n = 7).

Aiming to evaluate the performance of the micro-cartridge in the [^{18}F]fluoride pre-concentration process at production activities, conducted in a hot cell, Table 2 presents the efficiency results at activities greater than 110 GBq in a 2.5 mL volume of material produced in the cyclotron.

As shown in Table 2, the micro-cartridge exhibited remarkable efficiency in both the trapping (TE) and recovery (RE) stages, with average values of (91.5 ± 2.9)% and (93.9 ± 1.8)%, respectively. A detailed examination of the data revealed a slight variation in the TE, particularly in the initial test. This variation was attributed to the initial

Table 1 Results of trapping and recovery efficiency (TE and RE) of [^{18}F]fluoride for the tests in intermediate activity using only 1.5 mL of material produced in the cyclotron

Test	Activity	Micro-cartridge		
	(GBq)	TE (%)	RE (%)	QMA mass (mg)
1	0.1	100.0	100.0	6.5
2	1.2	99.0	98.9	7.0
3	2.2	98.4	99.9	6.3
4	2.7	98.8	98.8	7.9
5	3.0	98.4	98.9	8.0
6	8.9	99.3	98.9	6.1
7	9.5	99.0	99.7	7.5

Table 2 TE and RE efficiency results of [^{18}F]fluoride for conductive production activity in hot cell

Test	Activity	Micro-cartridge		
	(GBq)	TE (%)	RE (%)	QMA mass (mg)
1	110.2	88.9	97.1	7.6
2	120.7	90.9	93.0	8.2
3	122.8	92.1	93.8	7.9
4	123.9	94.2	94.0	8.1

pressure flow of (10.2 ± 0.3) psi, which may have limited the interaction of [^{18}F]fluoride with the anion exchange resin of the micro-cartridge due to the specific experimental arrangement of the hot cell. This configuration included the use of a long flexible tube ~ 150 cm in length (tests ≤ 10 GBq the length was ~ 25 cm) as the liquid inlet of the micro-cartridge, thereby facilitating its manipulation to the hot cell detector for activity measurements at each step.

To optimize the process, the pressure was set to (7.5 ± 0.3) psi in subsequent tests, resulting in an improvement in TE. The pressure for liquid displacement in the elution stage was maintained at (1.1 ± 0.3) psi. The average time for the entire pre-concentration process, including the displacement and removal of liquid between each stage, was (10.5 ± 1.0) minutes.

A comparison of the recovery efficiency of the micro-cartridge between the results of Table 1. Table 2 reveals a small discrepancy in the average RE for tests with activities above 110 GBq. Because activity level and gas flow rate/pressure were both increased in these high-activity trials, it is not possible to conclusively attribute the slight decrease in RE to one factor alone. Nevertheless, visual observation suggests that droplet formation and retention are more pronounced at higher activity levels, hinting that the activity amount is the key driver. Future fluid dynamics studies could isolate these variables to confirm their respective roles.

In addition, two conceptual tests were performed with activities of 1.6 GBq and 103.6 GBq. These tests were performed with a 50% decrease in elution (50 µL total), retaining a 5% water fraction (2.5 µL H_2O). For the lowest activity test, the micro-cartridge gave an RE of 98.0%, a result very similar to the previous ones (Table 1). However, for the test with an activity of 103.6 GBq, the recovery step achieved an RE of 54.9%, showing a significant reduction. In line with previous findings (Ovdiichuk et al. 2024), the reduced volume may yield a more concentrated [^{18}F]fluoride solution and thus could affect RE at higher activities. This aspect has been discussed in previous studies that have investigated the influence of the percentage of water in the eluate (Lebedev et al. 2013; Chao et al. 2018; Lemaire et al. 2010), even at activities up to 37 GBq.

Radiosynthesis yield of [^{18}F]FMISO without azeotropic drying

The manual radiosynthesis began with an initial activity of 1.2 GBq (Test 2—Table 1). Following the recovery step using the micro-cartridge, a volume of 100 µL containing the [^{18}F]fluoride was collected directly into a 2 mL conical vial containing 10.4 µmol of the NITTP precursor dissolved in 400 µL of CH_3CN (ratio: Precursor/K_2CO_3 Base = 1.9).

The radiolabeling synthesis was conducted at 110 °C for 10 min in a 500 µL reaction mixture containing 99% CH_3CN and 1% H_2O. After synthesis, the radiolabeled sample was analyzed via HPLC to determine the RCC of [^{18}F]fluoride incorporation into the intermediate product (THP-protected [^{18}F]FMISO). The results (Fig. 4) demonstrated complete incorporation of the [^{18}F]fluoride recovered during the micro-cartridge elution step, resulting in a 100% RCC (Supplementary Fig. S8 and Table S4).

A subsequent synthesis performed under identical conditions with an initial activity of 2.7 GBq (Test 4—Table 1) also revealed an identical result in its HPLC analysis, as reported in Fig. 4a for the formation of the THP-protected [^{18}F]FMISO product with 100% RCC (Supplementary Fig. S7 and Table S3). In light of the aforementioned RCC result, hydrolysis was performed by adding 200 µL of 0.5 M HCl and heating the mixture at 100 °C for 5 min. After cooling, the solution was neutralized with 200 µL of 0.5 M NaOH. At the conclusion of this sequence, a sample was subjected to HPLC analysis to confirm deprotection and determine the isolation efficiency (IE) of [^{18}F]FMISO (Fig. 5). The analysis after deprotection indicated an EI above 80% in the synthesis of the radiopharmaceutical [^{18}F]FMISO (Fig. 5a). It is worth mentioning that this high yield was obtained without the hydrolysis step by azeotropic drying in acidic medium.

The radiopharmaceutical was purified by transferring the total volume of the liquid mixture to a sequence of conventional cartridges (Sep-Pak C18 and alumina), which were then washed with 5 mL of ultrapure water. All eluates from this stage were discarded as waste. Subsequently, the final product was eluted from the sequence of cartridges with 5 mL of a 10% ethanol solution in Milli-Q water and collected in a new vial. Once the deprotection and purification process was complete, the final product was subjected to analysis by HPLC to confirm the results. To confirm the results, a standard sample of [^{19}F]FMISO was also analyzed (Fig. 5c), confirming the retention time of the final radiolabeled product. HPLC analysis showed a single radioactive peak (Fig. 5b), indicating

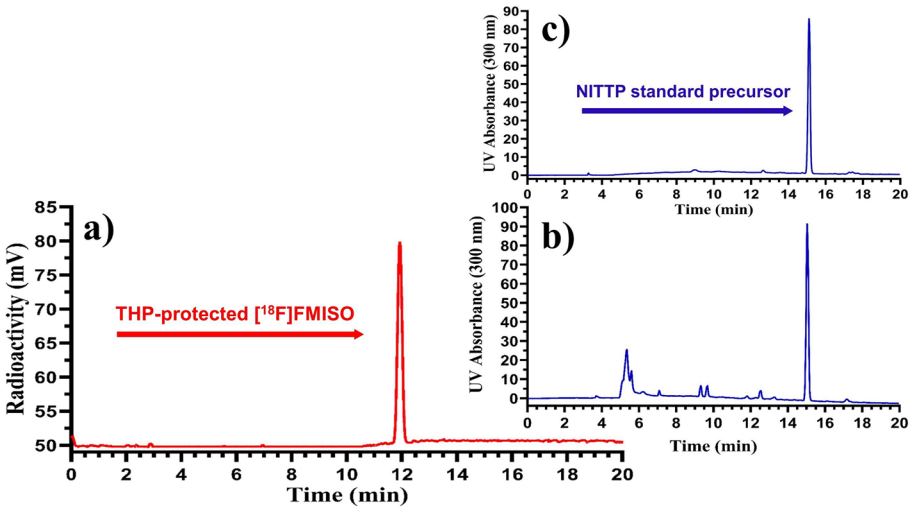

Fig. 4 HPLC analysis of THP-protected [^{18}F]FMISO with UV detection channel installed in front of the radioactivity detector: **a** Radioactivity detector TPH-protected [^{18}F]FMISO (Rt = 11.9 min); **b** UV channel analysis of THP-protected [^{18}F]FMISO **c** UV analysis for the NITTP standard precursor (Rt = 15.1 min Supplementary Fig. S9 and Table S5)

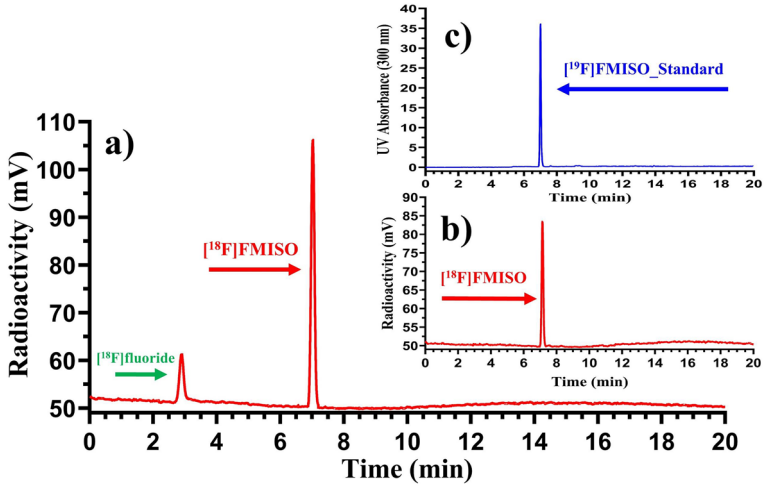

Fig. 5 HPLC analysis [^{18}F]FMISO: **a** Before purification, [^{18}F]FMISO (Rt = 7.0 min) showed an area of ~ 81%, while [^{18}F]fluorine (Rt = 3.3 min) showed an area of ~ 19% (Supplementary Fig. S10 and Table S6); **b** After purification of [^{18}F]FMISO (Rt = 7.1 min); **c** UV detector for the [^{19}F]FMISO standard (Rt = 6.9 min)

that no radioactive impurities were present (Supplementary Fig. S11 and Table S7). For the higher-activity run (2.7 GBq initial), purified [^{18}F]FMISO was obtained in a clear, colorless solution of ~ 5 mL after passage through C18 and alumina cartridges, free of any suspended particles. In contrast, attempts to reduce the elution volume to ~ 2 mL for a lower-activity run (1.2 GBq initial) led to incomplete recovery of [^{18}F]FMISO.

The entire manual synthesis process using the micro-cartridge was completed in 30 min. Based on the recovery efficiency (Tests 2 and 4 in Table 1), radiochemical conversion (RCC; n = 2), and incorporation efficiency (IE; n = 1), the overall corrected radiochemical yield (RCY) was estimated to be 78%. Although three radiolabeling assays were carried out, only two are discussed in detail here, reflecting the technical challenges encountered at lower activity with a smaller elution volume. These findings underscore the micro-cartridge's potential to obviate the need for azeotropic drying, a known source of activity losses in nucleophilic [^{18}F]fluoride reactions. Further studies will focus on optimizing purification conditions for varying initial activities and elution volumes.

Discussion

Some studies (Zhang et al. 2018a; Leonardis et al. 2011; Salvador et al. 2017) proposing the development of micro-cartridges have reported evaluations of TE and RE performance for the [^{18}F]fluoride pre-concentration process. In the work by De Leonardis et al. (Leonardis et al. 2011), a TE and RE of 95% were achieved with 0.9 GBq activity using eluent volumes ranging from 250 to 500 µL. Zhang et al. (2018a) reported TE of 95.9% and RE of 95.0% obtained in a test with 4.7 GBq activity and the recovery of [^{18}F]fluoride in a total eluent volume of 75 µL. Salvador et al. (2017) proposed a micro-cartridge with 53% RE for activities of 72.5 GBq and recovery of 67% of the activity in an eluate volume of up to 30 µL. In contrast to all these studies, our results for activities above 100 GBq demonstrated higher RE in all [^{18}F]fluoride recovery tests with 100 µL elution. Despite the total eluent volume used in our work being 1.3 (Zhang et al. 2018a) and 3.3 (Salvador

et al. 2017) times larger than reported by the other authors, our eluate contained only 5 µL of water and presented an RE of up to 97% in activities above 110 GBq.

Other studies in the literature (Elizarov et al. 2010; Lebedev et al. 2013; Chao et al. 2018), although not focusing on the development of micro-cartridges, but rather on microreactors for synthesis labeling using azeotropic drying, were also compare our TE and RE results in [^{18}F]fluoride pre-concentration. Elizarov et al. (2010), using a micro-cartridge with a 2 µL particle bed volume with a different resin than used in our research, achieved a TE of 99.5% with an initial activity of 32.4 GBq of [^{18}F]fluoride and a RE of 92.7% with an elution volume of 5 µL (only K_2CO_3 in water). Although our study employed a significantly larger total elution volume, the volume of water in the eluent is the same. Moreover, the [^{18}F]fluoride recovery results presented by the new micro-cartridge achieved a RE higher than 93.0% at activities ranging from two to nearly four times those used by Elizarov et al. (2010).

Labedev et al. (2013) and Chao et al. (2018) used micro-cartridges with particle bed volumes of 5 µL and 4 µL, respectively (both commercially produced by Optimize Technologies, Inc.), using the same anion exchange resin as (Elizarov et al. 2010). One of these studies reported that the micro-cartridge was able to trap 95% of the activities up to 111 GBq in the retention step. However, their experiments were conducted at 13.7 GBq activities, demonstrating a combined efficiency of TE and RE of (95 ± 3)%, using a total elution volume of 45 µL (33.3% water) (Lebedev et al. 2013). On the other hand (Chao et al. 2018), used 1.2 GBq (equivalent to 0.5 mL of cyclotron irradiated material), achieving a TE of 99% and RE of 96% of [^{18}F]fluoride in a total elution volume of 45 µL. Of these, 12.4 µL was an aqueous solution of K_3PO_4 and the remainder was CH_3CN used to rinse the micro-cartridge and improve the elution RE (Chao et al. 2018). Our results for activities up to 124 GBq showed an average trapping rate of (91.5 ± 2.2)%, with an RE of (93.9 ± 1.8)%. These are the first experimental results reported to date for the [^{18}F] fluoride recovery stage in micro-cartridges with activities above 110 GBq containing up to 5 µL of aqueous K_2CO_3 solution.

By adopting elution volumes equivalent to those used in previous studies (Lebedev et al. 2013; Chao et al. 2018), we obtained comparable results in terms of recovery efficiency for intermediate activities (1.6 GBq with RE of 98.0%), despite our micro-cartridge having a particle bed volume of only 17 µL. However, at higher activity levels (103.6 GBq with RE of 54.9%), a significant loss was observed in RE when using 50µL of eluent compared to the results obtained with 100µL, especially for activities above 107 GBq. This availability of water and the amount of K_2CO_3 (compared to 100 µL) in the elution solution, together with the high concentration of [^{18}F]fluoride at such high activity levels, negatively affects the RE, a factor highlighted in previous studies (Chao et al. 2018; Lemaire et al. 2010). Nevertheless, the water percentage in the eluate is crucial for eliminating the azeotropic drying step, as demonstrated by the labeling of various [^{18}F]fluoride radiopharmaceuticals on microfluidic platforms with this drying step suppressed (Ovdiichuk et al. 2024).

To date, there are no records of nucleophilic fluorination synthesis of [^{18}F]FMISO without the azeotropic drying step. Yokell et al. (2012), using the same microfluidic system as (Lebedev et al. 2013), reported results for the labeling of [^{18}F]FMISO using 5 mg of the precursor NITTP, with radiochemical yield (RCY) $\geq$ 56%, in a synthesis

time of 60 min. Also employing the microfluidic system, Zheng et al. (2015) demonstrated the formation of THP-protected [^{18}F]FMISO, with RCC ranging from 20 to 90% under different synthesis conditions (110 °C and 170 °C, respectively). According to the same authors, the RCY of the final synthesis was (28.4 ± 3.0)%, with a duration of (106 ± 11) minutes, using 0.4 mg of precursor mass.

When comparing the microfluidic-scale synthesis of THP-protected [^{18}F]FMISO without azeotropic drying to other studies (Zheng et al. 2015; Yokell et al. 2012), that also relied solely on radio-HPLC for RCC assessment, our analysis detected no measurable radioactive by-products, suggesting an RCC approaching 100% (n = 2). Furthermore, the radiolabeling time of THP-protected [^{18}F]FMISO was only 10 min at 110 °C, representing a significant reduction in time and lower temperature compared to that reported by the same authors.

In a recent study, Kniess et al. (2023), using the automated module for conventional synthesis (GE Healthcare's FASTlab®), presented synthesis results of [^{18}F]FMISO with the highest molar activity reported to date, 588 GBq/μmol, using 10 mg of precursor. The synthesis time was 48 min, and the final RCY was up to 49%. In contrast, in our study, when comparing the synthesis time only for the formation of THP-protected [^{18}F]FMISO with that of (Kniess et al. 2023), we achieved twice the efficiency by not employing azeotropic drying. This happens because the authors described that the time dedicated to the azeotropic drying step and the synthesis of THP-protected [^{18}F]FMISO labeling was 22 min.

Although our research did not focus on the final synthesis of [^{18}F]FMISO, it prioritized evaluating the recovery efficiency of the micro-cartridge at various activity levels, yielding encouraging results. An RCY of 78% was achieved in activity up to 2.7 GBq using manual synthesis. Given that azeotropic drying can lead to activity losses of up to ~ 30% (Haveman et al. 2023; Brichard and Aigbirhio 2014; Zhou et al. 2023), eliminating this step may help improve retention, as reported in the literature. Further studies are needed to explore its impact on large-scale clinical and commercial applications. However, the results of this study demonstrate that radiosynthesis of [^{18}F]FMISO using the micro-cartridge without azeotropic drying opens up the opportunity for hybrid processes using microfluidic technology with conventional synthesis kits for production, a trend pointed out in a recent study (Scott et al. 2024).

Conclusion

This study highlights the transformative potential of using advanced micro-cartridge technology for the pre-concentration and labeling of [^{18}F]fluoride in radiopharmaceutical production. The laser-fabricated micro-cartridge leveraged the ultrashort pulse etching process, enabling the manufacturing of a microfluidic device without altering the physicochemical properties of the substrate. Additionally, this process achieved excellent verticality of the walls between the micropillars. While the primary focus of this study is not the synthesis of [^{18}F]FMISO, the developed micro-cartridge was employed in the pre-concentration process of [^{18}F]fluoride. Its use in this process demonstrated the potential for the elimination of complex and time-consuming steps, such as azeotropic drying, which is used in most nucleophilic fluorination syntheses. The result is a simplified process and an overall increased radiolabeling efficiency. The successful application

of micro-cartridge synthesis paves the way for the integration of microfluidic technology with conventional synthesis modules, offering a path to more streamlined hybrid production processes. This advancement has the potential to enhance specific activity and synthesis yields while contributing to the development of more efficient radiopharmaceutical production processes, ultimately benefiting the field of nuclear medicine and patient care worldwide. Although our current micro-cartridge design is based on borosilicate glass (BK7) and laser micromachining, as reported for a single micro-cartridge, future developments could explore alternative and more affordable materials, using laser micromachined molds as a possible strategy for manufacturing scalability. Future studies will focus on quantifying production costs, optimizing the choice of alternative materials, and evaluating the best strategies for high-throughput manufacturing of the micro-cartridge.

Abbreviations

[^{18}F]FMISO	[^{18}F]Fluoromisonidazole
^{15}O	Oxygen-15
BK7	Borosilicate optical glass
HPLC	High performance liquid chromatography
IE	Isolation efficiency
NITTP	1-(2′-Nitro-1′-imidazolyl)-2-O-tetrahydropyranyl-3-O-tosyl-propanediol
PDMS	Polydimethylsiloxane
PET	Positron emission tomography
RCC	Radiochemical conversion
RCY	Radiochemical yield
RE	Recovery efficiency
TE	Trapping efficiency
Rt	Retention time

Supplementary Information

The online version contains supplementary material available at https://doi.org/10.1186/s41181-025-00334-x.

Additional file 1.

Acknowledgements
The staff at Radiopharmacy Center, Cyclotron Accelerator Centers and Laser and Applications Center, at Nuclear and Energy Research Institute, São Paulo, Brazil are acknowledged for technical assistance.

Author contributions
All authors read and approved the final manuscript. Conceptualization AAG, APN and WR; methodology, AAG, APN and ALL; writing—original draft preparation, AAG, ESB and RES; writing—review and editing, all authors; funding acquisition, ESB and WR.

Funding
The authors would like to acknowledge the financial support for this research by the following organizations and projects: CNPq—INCTs (INFO-465763/2014-6, INTERAS-406761/2022-1), CNPq (Sisfóton-440228/2021-2, GD 174673/2023-0), Project COPDE/IPEN 2020.06.08, FAPESP-2013-26113-6 and CAPES (Finances Code 001, PROEX 88887.595780/2020-00).

Availability of data and materials
The datasets used and/or analyzed during the current study are available from the corresponding author upon reasonable request.

Declarations

Ethics approval and consent to participate
Not applicable.

Consent for publication
Not applicable.

Competing interests
The authors declare that they have no competing interests.

Received: 6 January 2025 Accepted: 27 February 2025
Published online: 21 March 2025

References

Arima V, Pascali G, Lade O, Kretschmer HR, Bernsdorf I, Hammond V, et al. Radiochemistry on chip: Towards dose-on-demand synthesis of PET radiopharmaceuticals. Lab Chip. 2013;13(12):2328–36.
Baker CA, Bulloch R, Roper MG. Comparison of separation performance of laser-ablated and wet-etched microfluidic devices. Anal Bioanal Chem. 2011;399(4):1473–9.
Berg E, Cherry SR. Innovations in instrumentation for positron emission tomography. Sem Nucl Med. 2018;48(4):311–31. https://doi.org/10.1053/j.semnuclmed.2018.02.006.
Brichard L, Aigbirhio FI. An efficient method for enhancing the reactivity and flexibility of [^{18}F]fluoride towards nucleophilic substitution using tetraethylammonium bicarbonate. Eur J Org Chem. 2014;2014(28):6145–9.
Chao PH, Lazari M, Hanet S, Narayanam MK, Murphy JM, van Dam RM. Automated concentration of [^{18}F]fluoride into microliter volumes. Appl Radiat Isot. 2018;141:138–48. https://doi.org/10.1016/j.apradiso.2018.06.017.
De Leonardis F, Pascali G, Salvadori PA, Watts P, Pamme N. On-chip pre-concentration and complexation of [^{18}F]fluoride ions via regenerable anion exchange particles for radiochemical synthesis of Positron Emission Tomography tracers. J Chromatogr A. 2011;1218(29):4714–9. https://doi.org/10.1016/j.chroma.2011.05.062.
Elizarov AM, Van Dam RM, Shin YS, Kolb HC, Padgett HC, Stout D, et al. Design and optimization of coin-shaped microreactor chips for PET radiopharmaceutical synthesis. J Nucl Med. 2010;51(2):282–7.
Elsinga P, Todde S, Penuelas I, Meyer G, Farstad B, Faivre-Chauvet A, et al. Guidance on current good radiopharmacy practice (cGRPP) for the small-scale preparation of radiopharmaceuticals. Eur J Nucl Med Mol Imaging. 2010;37(5):1049–62.
Gomes AA, Vianna A dos S, de Arruda Morreira G, Landufo E, Samad RE, Bernardes ES, et al. (2022) Determination of parameters for micromachining of microfluidic mixers with complex geometry in glass using ultra-short laser pulse. In: Latin America Optics and Photonics (LAOP) Conference. Washington, D.C.: Optica Publishing Group; 2022. pp M4C.2. Available from: https://opg.optica.org/abstract.cfm?URI=LAOP-2022-M4C.2
Gomes AA, Nario AP, Lapolli AL, Samad RE, Bernardes ES, de Rossi W. (2024) Micro-cartridge applied to Fluorine-18 concentration developed with ultrashort laser pulse machining. In: Optica latin America optics and photonics conference (LAOP) 2024 [Internet]. Washington, D.C.: Optica Publishing Group; pp M4C.6. Available from: https://opg.optica.org/abstract.cfm?URI=LAOP-2024-M4C.6
Hamacher K, Coenen HH, Stocklin G. Efficient stereospecific synthesis of no-carrier-added 2-[^{18}F]-Fluoro-2-deoxy-d-glucose using aminopolyether supported nucleophilic substitution. J Nucl Med. 1986;27:235–8.
Haveman LYF, Vugts DJ, Windhorst AD. State of the art procedures towards reactive [^{18}F]fluoride in PET tracer synthesis. EJNMMI Radiopharm Chem. 2023;8(1):28. https://doi.org/10.1186/s41181-023-00203-5.
Herth MM, Ametamey S, Antuganov D, Bauman A, Berndt M, Brooks AF, et al. On the consensus nomenclature rules for radiopharmaceutical chemistry—reconsideration of radiochemical conversion. Nucl Med Biol. 2021;93:19–21. https://doi.org/10.1016/j.nucmedbio.2020.11.003.
Hoover AJ, Lazari M, Ren H, Narayanam MK, Murphy JM, Van Dam RM, et al. A Transmetalation reaction enables the synthesis of [^{18}F]5-fluorouracil from [^{18}F]fluoride for human PET imaging. Organometallics. 2016;35(7):1008–14.
Jacobson O, Kiesewetter DO, Chen X. Fluorine-18 radiochemistry, labeling strategies and synthetic routes. Bioconjug Chem. 2015;26(1):1–18.
Juodenas M, Tamulevičius T, Ulčinas O, Tamulevičius S. Implementation of an optimized microfluidic mixer in alumina employing femtosecond laser ablation. J Micromech Microeng. 2018;28(1):015013.
Kämäräinen EL, Kyllönen T, Nihtilä O, Björk H, Solin O. Preparation of fluorine-18-labelled fluoromisonidazole using two different synthesis methods. J Label Compd Radiopharm. 2004;47(1):37–45.
Knapp KA, Nickels ML, Manning HC. The current role of microfluidics in radiofluorination chemistry. Mol Imaging Biol. 2020;22(3):463–75.
Kniess T, Zessin J, Mäding P, Kuchar M, Kiss O, Kopka K. Synthesis of [^{18}F]FMISO, a hypoxia-specific imaging probe for PET, an overview from a radiochemist's perspective. EJNMMI Radiopharm Chem. 2023;8(1):5.
Krasikova R. Synthesis modules and automation in F-18 labeling. Ernst Schering Res Found Workshop. 2007;62:289–316.
Lebedev A, Miraghaie R, Kotta K, Ball CE, Zhang J, Buchsbaum MS, et al. Batch-reactor microfluidic device: first human use of a microfluidically produced PET radiotracer. Lab Chip. 2013;13(1):136–45.
Lee C-C, Sui G, Elizarov A, Shu CJ, Shin Y-S, Dooley AN, et al. Multistep synthesis of a radiolabeled imaging probe using integrated microfluidics. Science. 2005;310(5755):1793–6. https://doi.org/10.1126/science.1118919.
Lemaire CF, Aerts JJ, Voccia S, Libert LC, Mercier F, Goblet D, et al. Fast production of highly reactive no-carrier-added [^{18}F] Fluoride for the labeling of radiopharmaceuticals. Angew Chemie. 2010;122(18):3229–32.
Lisova K, Wang J, Hajagos TJ, Lu Y, Hsiao A, Elizarov A, et al. Economical droplet-based microfluidic production of [^{18}F]FET and [^{18}F]Florbetaben suitable for human use. Sci Rep. 2021;11(1):1–12. https://doi.org/10.1038/s41598-021-99111-4.
Machado LM, Samad RE, Freitas AZ, Vieira ND, De Rossi W. Microchannels direct machining using the femtosecond smooth ablation method. Phys Procedia. 2011;12(2):67–75. https://doi.org/10.1016/j.phpro.2011.03.107.
Machado LM, Samad RE, de Rossi W, Junior NDV. D-Scan measurement of ablation threshold incubation effects for ultrashort laser pulses. Opt Express. 2012;20(4):4114.
Niculescu AG, Chircov C, Bîrcă AC, Grumezescu AM. Fabrication and applications of microfluidic devices: a review. Int J Mol Sci. 2021;22(4):1–26.
Nolte S, Schrempel F, Dausinger F, editors. Ultrashort Pulse Laser Technology: Laser Sources and Applications. Cham: Springer International Publishing; 2016.

Ovdiichuk O, Mallapura H, Pineda F, Hourtané V, Långström B, Halldin C, et al. Implementation of iMiDEV™, a new fully automated microfluidic platform for radiopharmaceutical production. Lab Chip. 2021;21(11):2272–82. https://doi.org/10.1039/D1LC00148E.
Ovdiichuk O, Lahdenpohja S, Béen Q, Tanguy L, Kuhnast B, Collet-Defossez C. [^{18}F]fluoride activation and ^{18}F-labelling in hydrous conditions—towards a microfluidic synthesis of PET radiopharmaceuticals. Molecules. 2024;29(1):147.
Panigrahi PK. Transport Phenomena in Microfluidic Systems. Singapore: John Wiley & Sons Singapore Pte; 2016. p. 1–514. https://doi.org/10.1002/9781118298428.
Pascali G, Nannavecchia G, Pitzianti S, Salvadori PA. Dose-on-demand of diverse ^{18}F-fluorocholine derivatives through a two-step microfluidic approach. Nucl Med Biol. 2011;38(5):637–44. https://doi.org/10.1016/j.nucmedbio.2011.01.005.
Pascali G, Watts P, Salvadori PA. Microfluidics in radiopharmaceutical chemistry. Nucl Med Biol. 2013;40(6):776–87.
Pascali G, Simone M, Matesic L, Greguric I, Salvadori P. Tolerance of water in microfluidic radiofluorinations: a potential methodological shift. J Flow Chem. 2014;4(2):86–91.
Patt M, Kuntzsch M, Machulla HJ. Preparation of [^{18}F]fluoromisonidazole by nucleophilic substitution on THP-protected precursor: yield dependence on reaction parameters. J Radioanal Nucl Chem. 1999;240(3):925–7.
Pawar P, Ballav R, Kumar A. Micromachining of borosilicate glass: a state of art review. Mater Today Proc. 2017;4(2):2813–21. https://doi.org/10.1016/j.matpr.2017.02.161.
Pees A, Sewing C, Vosjan MJWD, Tadino V, Herscheid JDM, Windhorst AD, et al. Fast and reliable generation of [^{18}F]triflyl fluoride, a gaseous [^{18}F]fluoride source. Chem Commun. 2018;54(72):10179–82.
Rahmim A, Zaidi H. Pet versus spect: strengths, limitations and challenges. Nucl Med Commun. 2008;29(3):193–207.
Salvador B, Luque A, Fernandez-Maza L, Corral A, Orta D, Fernández I, et al. Disposable PDMS chip with integrated [^{18}F] fluoride pre-concentration cartridge for radiopharmaceuticals. J Microelectromechanical Syst. 2017;26(6):1442–8.
Scott PJH, editor. Radiochemical syntheses: further radiopharmaceuticals for positron emission tomography and new strategies for their production. Wiley; 2015. https://doi.org/10.1002/9781118834114.
Scott PJ, Penuelas I, Rey A, Aime S, Ambikalmajan PMR, Antunes IF, et al. Highlight selection of radiochemistry and radiopharmacy developments by editorial board. EJNMMI Radiopharm Chem. 2024;9(1):67. https://doi.org/10.1186/s41181-024-00296-6.
Shakeri A, Jarad NA, Leung A, Soleymani L, Didar TF. Biofunctionalization of glass- and paper-based microfluidic devices: a review. Adv Mater Interfaces. 2019;6(19):1900940. https://doi.org/10.1002/admi.201900940.
Sorger D, Patt M, Kumar P, Wiebe LI, Barthel H, Seese A, et al. [^{18}F]Fluoroazomycinarabinofuranoside (^{18}FAZA) and [^{18}F] Fluoromisonidazole (^{18}FMISO): a comparative study of their selective uptake in hypoxic cells and PET imaging in experimental rat tumors. Nucl Med Biol. 2003;30(3):317–26.
Sushanta K, Mitra SC. Microfluidics and Nanofluidics Handbook. In: Mitra SK, Chakraborty S, editors. Inventions. Boca Raton: CRC Press; 2012.
Vallabhajosula S. 18F-labeled positron emission tomographic radiopharmaceuticals in oncology: an overview of radiochemistry and mechanisms of tumor localization. Semin Nucl Med. 2007;37(6):400–19.
Vallabhajosula S. Molecular Imaging. Neuroimaging in Schizophrenia. Berlin, Heidelberg: Springer, Berlin Heidelberg; 2009. p. 145–59. https://doi.org/10.1007/978-3-540-76735-0.
Waldbaur A, Rapp H, Länge K, Rapp BE. Let there be chip—towards rapid prototyping of microfluidic devices: one-step manufacturing processes. Anal Methods. 2011;3(12):2681–716.
Yokell DL, Leece AK, Lebedev A, Miraghaie R, Ball CE, Zhang J, et al. Microfluidic single vessel production of hypoxia tracer 1H–1-(3-[^{18}F]-fluoro-2-hydroxy-propyl)-2-nitro-imidazole ([^{18}F]-FMISO). Appl Radiat Isot. 2012;70(10):2313–6. https://doi.org/10.1016/j.apradiso.2012.05.022.
Yu S. Review of ^{18}F-FDG synthesis and quality control. Biomed Imag Interv J. 2006;2(4):e57.
Zhang X, Liu F, Knapp KA, Nickels ML, Manning HC, Bellan LM. A simple microfluidic platform for rapid and efficient production of the radiotracer [^{18}F]fallypride. Lab Chip. 2018a;18(9):1369–77. https://doi.org/10.1039/C8LC00167G.
Zhang B, Pascali G, Wyatt N, Matesic L, Klenner MA, Sia TR, et al. Synthesis, bioconjugation and stability studies of [^{18}F] ethenesulfonyl fluoride. J Label Compd Radiopharm. 2018b;61(11):847–56.
Zhang B, Fraser BH, Klenner MA, Chen Z, Liang SH, Massi M, et al. [^{18}F]Ethenesulfonyl fluoride as a practical radiofluoride relay reagent. Chem A Eur J. 2019;25(32):7613–7.
Zhang M, Li S, Zhang H, Xu H. Research progress of ^{18}F labeled small molecule positron emission tomography (PET) imaging agents. Eur J Med Chem. 2020;205:112629. https://doi.org/10.1016/j.ejmech.2020.112629.
Zheng MQ, Collier L, Bois F, Kelada OJ, Hammond K, Ropchan J, et al. Synthesis of [^{18}F]FMISO in a flow-through microfluidic reactor: development and clinical application. Nucl Med Biol. 2015;42(6):578–84.
Zhou D, Chu W, Xu J, Schwarz S, Katzenellenbogen JA. [^{18}F]Tosyl fluoride as a versatile [^{18}F]fluoride source for the preparation of ^{18}F-labeled radiopharmaceuticals. Sci Rep. 2023;13(1):3182. https://doi.org/10.1038/s41598-023-30200-2.

Publisher's Note